

Effect of Temperature on Optical Properties of Nanocrystalline Ceramics $\text{Fe}_2\text{Mn}_2\text{Ni}_2\text{Zn}_2\text{O}_{11}$

Anitha S Nair¹, Jayakumari Isac²

¹Department of Physics, D.B College, Parumala, Kerala, India

²Centre for Condensed Matter, Department of Physics, CMS College, Kottayam, India

Abstract: *In this article the effect of temperature on optical properties of nanocrystalline ceramic Ferromanganese nickel zinc oxide $\text{Fe}_2\text{Mn}_2\text{Ni}_2\text{Zn}_2\text{O}_{11}$ were studied. Using the Tauc gap, the absorption spectrum method was applied to estimate the optical band gap. The sample was synthesized thermo chemically by solid state method at different treating temperatures. A characteristic feature of all solid-state reactions is that they involve the formation of product phase(s) at the interfaces of the reactants. UV-VIS analysis of the sample was carried out. The optical constants of refractive index, extinction coefficient, normal-incidence reflectivity, and absorption coefficient showed systematic variation with temperature. From these data the absorption coefficient was calculated and the band gap energy was determined. Using the Wemple- Di Domenico single-oscillator model the dispersion of refractive index was analyzed. From these data, the absorption coefficients were calculated and the band gap energy determine*

Keywords: Absorption spectrum, band gap energy, Dispersion, $\text{Fe}_2\text{Mn}_2\text{Ni}_2\text{Zn}_2\text{O}_{11}$, Wemple-DiDomenico model, Extinction coefficient.

1. Introduction

There is a growing interest in nanocrystalline materials because of their remarkable properties when they are compared to the parent bulk solids. Reasons for the interest in nanocrystalline oxides include the possibilities of producing superhard and superplastic ceramics and catalysts with enhanced activities.

Optical gap is different from the quasi-particle gap (at least in the conventional BCS theory for bulk materials, the superconducting gap coincides with the quasi-particle gap arising from pairing). In optical experiments (Tauc plot is used for determining optical gap) one excites particles that remain to interact with the hole they leave behind; in contrast, in photo-emission (and inverse photo-emission) experiments, one truly removes (adds) particles from (to) systems. The optical gap is in general smaller than the quasi-particle gap, the difference being the binding energy of the bound states that electrons can form with holes (forming excitons). This binding energy can be small, whereby optical gap can be very close to the quasi-particle gap, but this is not in general the case. Incidentally, because bound states cannot be calculated by means of finite-order perturbation theory, calculation of the optical gap in general requires solving the relatively complicated Bethe-Salpeter equations [1]. In the present work the authors describes the optical behaviour of $\text{Fe}_2\text{Mn}_2\text{Ni}_2\text{Zn}_2\text{O}_{11}$ a nanocrystalline superconductor material. The energy band gap values of the sample were analyzed for different temperatures and they are fundamentally important to the design of practical devices [2]. In solid-state physics, a band gap, also called an energy gap or band gap, is an energy range in a solid where no electron states can exist. In graphs of the electronic band structure of solids, the band gap generally refers to the energy difference (in electron volts) between the top of the valence band and the bottom of the conduction band in insulators and semiconductors. This is equivalent to the energy required to free an outer shell electron from its orbit about the nucleus to become a mobile charge carrier, able to

move freely within the solid material, so the band gap is a major factor determining the electrical conductivity of a solid. Substances with large band gaps are generally insulators, those with smaller band gaps are semiconductors, while conductors either have very small band gaps or none, because the valence and conduction bands overlap [3].

Measuring the band gap is an important factor determining the electrical conductivity in nano material industries. A Tauc plot is used to determine the optical gap, or Tauc gap, in semiconductors. The Tauc gap is often used to characterize practical optical properties of amorphous materials [4]. The band gap energy values obtained using Tauc plot showed a direct relation with temperature. The optical constants of refractive index, extinction coefficient, and absorption coefficient showed a systematic variation with temperature. The dispersion of refractive index was analyzed by the Wemple-DiDomenico single-oscillator model and such optical behaviour is rarely reported. The Urbach energy of the sample was also studied.

2. Experimental

Nanocrystalline $\text{Fe}_2\text{Mn}_2\text{Ni}_2\text{Zn}_2\text{O}_{11}$ ceramics with the chemical formula was prepared by the solid state reaction technique according to the molecular formula. The powders of the required ceramics were mixed mechanically. Manganese oxide, nickel oxide, zinc oxide, ferric oxide powders were used as the raw materials [5]. Then the material calcined at different treating temperatures, 30⁰C, 500⁰C, 800⁰C and 950⁰C. Control of temperature is often necessary to ensure that the desired crystalline phase is formed with optimum particle size [6]. Then UV-Vis spectrum of these materials was taken. The dispersion of refractive index was analyzed by the Wemple- Di Domenico single-oscillator model. The optical constants of refractive index, extinction coefficient, normal-incidence reflectivity, and absorption coefficient showed systematic variation with temperature.

2.1. UV-VIS. Analysis

UV-Vis. spectroscopy was used to characterize the optical absorption properties [7]. The optical absorption spectrum of the sample was studied at room temperature. The optical absorption data were analyzed using the classical relation for near edge optical absorption of semiconductors [8-9]. The UV-Vis absorption spectra of the samples were recorded in the wavelength range of 200 to 800 nm using a Shimadzu UV 3600 UV-VIS-NIR spectrometer (Shimadzu Corporation, Kyoto, Japan) in diffuse reflectance mode. Spectra were recorded at room temperature, and the data were transformed through the Kubelka-Munk function [7]. This type of sample has high mechanical hardness, high thermal conductivity, large dielectric constant, and high resistance to harsh environment. UV-Visible spectrum gives information about the excitonic and inter transition of nano materials [10]. Figure.1 shows the UV-VIS behaviour of the sample $\text{Fe}_2\text{Mn}_2\text{Ni}_2\text{Zn}_2\text{O}_{11}$ at 950°C .

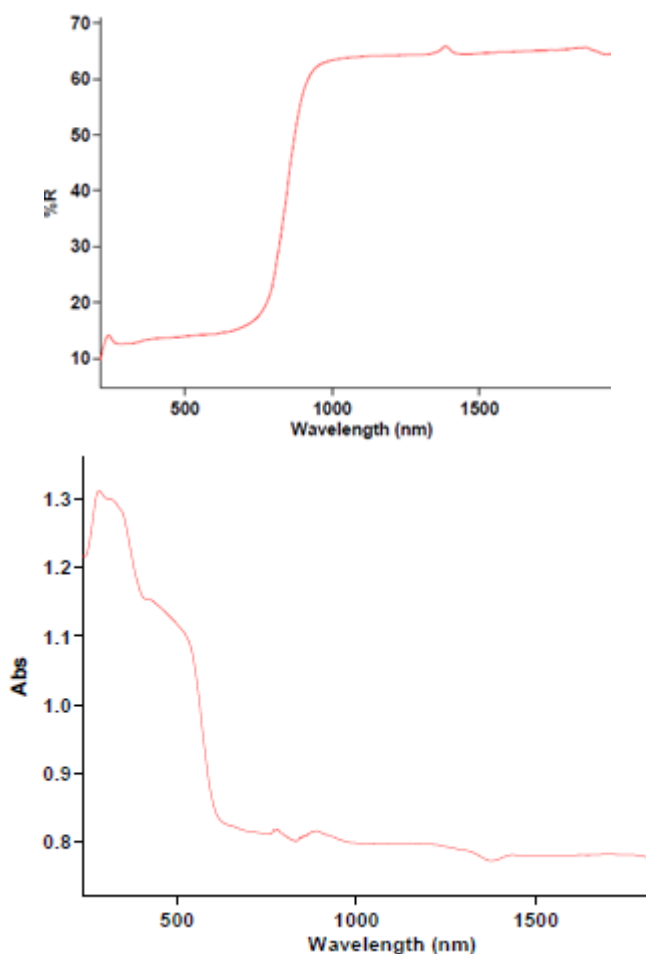


Figure 1: UV-VIS. Spectrum of $\text{Fe}_2\text{Mn}_2\text{Ni}_2\text{Zn}_2\text{O}_{11}$ (reflectance & absorbance)

The diffuse reflectance spectra were translated into the absorption spectra by the Kubelka-Munk method. Kubelka-Munk's equation is described as follows:

$$\alpha = (1-R)^2/2R - (1), \text{ where } \alpha \text{ is the absorption coefficient and } R \text{ the reflectivity at a particular wavelength [11].}$$

A Tauc plot is a convenient way of displaying the optical absorption spectrum of a material, pioneered by Jan Tauc, who proved that momentum is not conserved even in a direct optical transition. Typically, a Tauc plot shows the quantity $h\nu$ (the energy of the light) on the abscissa and the quantity $(\alpha h\nu)^{1/r}$ on the ordinate, where α is the absorption coefficient of the material. The value of the exponent r denotes the nature of the transition: $r = 1/2$ for direct allowed transitions $r = 3/2$ for direct forbidden transitions $r = 2$ for indirect allowed transitions $r = 3$ for indirect forbidden transitions. The resulting plot has a distinct linear regime which denotes the onset of absorption. Thus, extrapolating this linear region to the abscissa yields the energy of the optical band gap of the material [4]. According to the Tauc relation, the absorption coefficient α for a material is given by $\alpha = A(h\nu - E_g)^n$, Where E_g the band gap, constant A is different for different transitions, $(h\nu)$ is energy of photon in eV and n denotes the nature of the sample transition [12]. Optical absorption and luminescence occur by transition of electrons and holes between electronic states (bands, tail states, gap states). If electron-phonon coupling is strong enough that self-trapping occurs.

Absorption coefficient α is defined by $I(z) = I_0 \exp \{-\alpha z\}$ where $I(z)$ is the flux density if incident light is I_0 , z is the distance measured from the incident surface. Hence $\alpha = -(1/I(z)) dI(z)/dz$

Tauc law (Tauc plot, A region)

The absorption coefficient, α , due to inter band transition near the band-gap is well described: $\alpha h\omega = B (h\omega - E_g)^2$, $h\omega$ is photon energy, E_g is optical gap. This Tauc plot defines the optical gap in amorphous semiconductors.

(B region)

The absorption coefficient at the photon energy below the optical gap (tail absorption) depends exponentially on the photon energy $\alpha(h\omega) \sim \exp (h\omega/E_u)$, where E_u is called Urbach energy

C region

In addition, optical absorption by defects also appears at energy lower than optical gap. Likewise α is written as another exponential function of photon energy: $\alpha(h\omega) \sim \exp (h\omega/E_d)$, E_d belongs to the width of the defect states. C region is rather sensitive to the structural properties of materials [13]. The edge arises due to a radioactive recombination between trapped electrons and trapped holes in tail and gap states as shown in Fig.2, and is dependent on the degree of structural and thermal disorder [14]. The TAUC plot of a sample defines the optical band gap as the region A in fig.2. The tauc plot of the sample is given in Fig 5. It is reported that optical gap energy of nano-sized crystal depends on its crystallite size, it increases with decreasing crystallite size in the nano size range [15-16]. The extinction coefficient and the absorption coefficient are related as $\alpha(E) = 4\pi/\lambda (k(E))$ —(3). Variation of band gap energy with samples annealed at different temperatures is shown in figure 4. The natural logarithm of the absorption coefficient, $\alpha(\nu)$, was plotted as a function of the photon energy, $h\nu$ (Fig.7). The value of E_u was calculated by taking the reciprocal of the slopes of the linear portion in the lower photon energy region of curves. The measurement of

temperature-dependent Urbach tails distinguishes a temperature-dependent tail and a temperature-independent part, which mainly are due to intrinsic defects. The latter can be controlled by improving the crystal growth and the purity of the ingredients. The temperature-dependent part of the Urbach tail, is purely of intrinsic reasons [17].

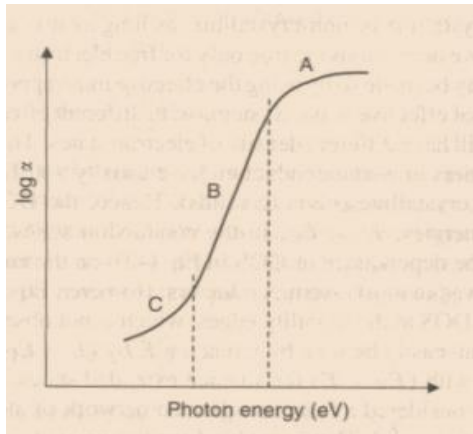


Figure 2: Optical band gap energy variation with absorption.

The absorption coefficient at the photon energy below the optical gap (tail absorption) depends exponentially on the photon energy: $\alpha(h\nu) \sim \exp(-h\nu/E_u)$ (4) where E_u is called Urbach energy. The region B in the fig.2 represents the Urbach energy. The absorption edge called the Urbach energy, depends on temperature, thermal vibrations in the lattice, induced disorder, static disorder, strong ionic bonds and on average photon energies [18]. The edge arises due to a radioactive recombination between trapped electrons and trapped holes in tail and gap states as shown in Fig.2, and is dependent on the degree of structural and thermal disorder [19].

It is observed in many cases that optical absorption by defects also appears at energy lower than optical gap (region C of fig.2). This region is related to the structural properties of materials [20]. Fig.3 helps us to reach the Band gap energy.

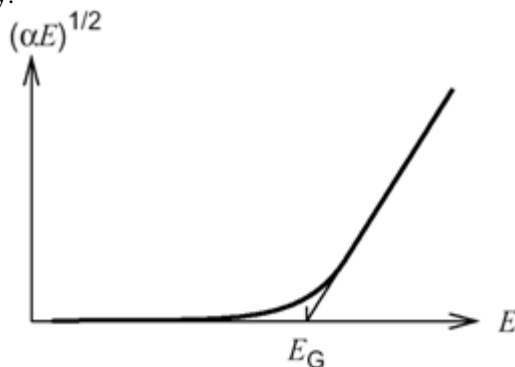


Figure 3: Band gap energy calculation

2.2. Refractive Index and Dispersion

There is a change in refractive index with wavelength. The refractive index values show a linear decrease with the increase in wavelength, Fig.7 shows the variation of the dispersion curve with annealing temperatures. The refractive

index and dispersion is expressed as equation of Di Domenico as $n^2 - 1 = E_d E_0 / (E_d^2 - (h\nu)^2)$ (5) where n is the refractive index, h is Planck's constant, ν is the frequency, $h\nu$ is the photon energy, E_0 is the average excitation energy for electronic transitions and E_d is the dispersion energy which is the measure of the strength of inter band optical transitions. The dielectric response for transitions below the optical gap is described by this model. E_0 and E_d values were calculated from the slope and intercept on the vertical axis of plot of $1/(n^2 - 1)$ versus $(h\nu)^2$ [21]. The static refractive index $n(0)$ at zero photon energy is evaluated from Equation (5), i.e. $n^2(0) = 1 + E_d/E_0$ (6) [22]. The dependence of extinction coefficient (k) on the wavelength is shown in Figure. The Figure shows an increase in k value with increasing wavelength.

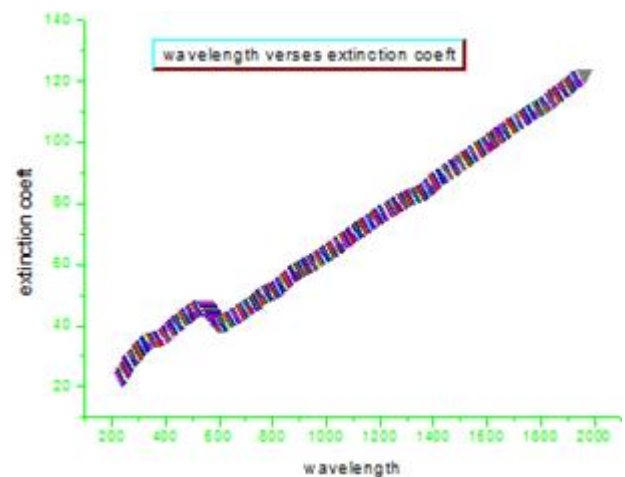


Figure 4: Extinction coefficient varies with wavelength

The extinction coefficient can be calculated by the relation $k = \alpha \lambda / 4\pi$. Where λ is the wavelength, α is the absorption coefficient. The refractive index of the films was calculated by the following equation $n = \{ (4R/(R-1)^2 - K^2) - (R-1)/(R-1) \}^{1/2}$ where R the reflectance and k the extinction coefficient [21]. Refractive index value shows a slight increase with increasing annealing temperature and attains a fixed value after a particular wavelength. The refractive index values showed a linear decrease with the increase in wavelength when plotted with refractive index along the Y-axis & wavelength along the X axis (figure 8).

3. Results and Discussion

The optical analysis of the ceramic material prepared by solid state reaction technique and treated at different temperatures is successfully done using UV-Vis Spectrophotometer. UV-VIS analysis, clearly confirms that band gap energy of the nano ceramic increases as the annealing temperature of the sample is increased. Here the direct allowed transitions are considered. The calculated value of the band gap energy of the sample at different values of temperature is given in table -1.

The Tauc plot is plotted with $h\nu$ along the X-axis and $(h\nu a)^2$ along the Y-axis. The band gap at a particular temperature is found by extrapolating the X axis. The Tauc plot of the sample at temperatures 950°C is given in Fig.5. From the graph the band gap energy values of $Fe_2Mn_2Ni_2Zn_2O_{11}$ at

different temperatures are noted and tabulated as given below (Table-1).

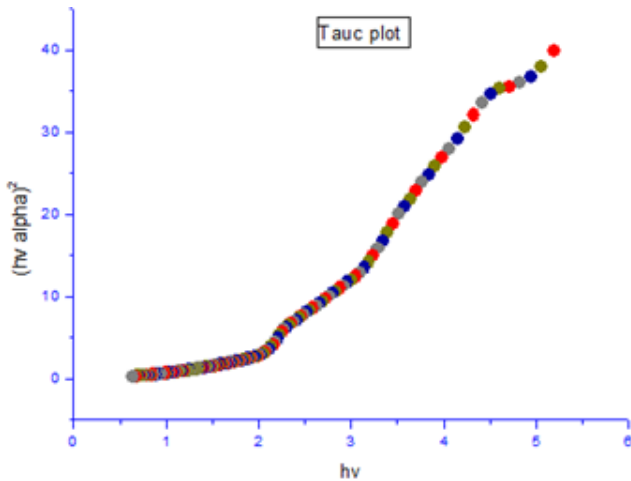


Figure 5: The Tauc plot of $\text{Fe}_2\text{Mn}_2\text{Ni}_2\text{Zn}_2\text{O}_{11}$

Table 1: Band gap energy values of $\text{Fe}_2\text{Mn}_2\text{Ni}_2\text{Zn}_2\text{O}_{11}$ at different temperatures

Temperature	Band gap energy in eV
30°C	1.28
500°C	1.34
800°C	1.71
950°C	2.24

Fig.6. shows the variation of band gap energy with increase in annealing temperature of the sample. The energy levels are dependent on the degree of structural order–disorder in the lattice. The band gap increases with the crystallite size but decreases as the perovskite phase is formed which proves the quantum confinement also decreasing its dislocation density.

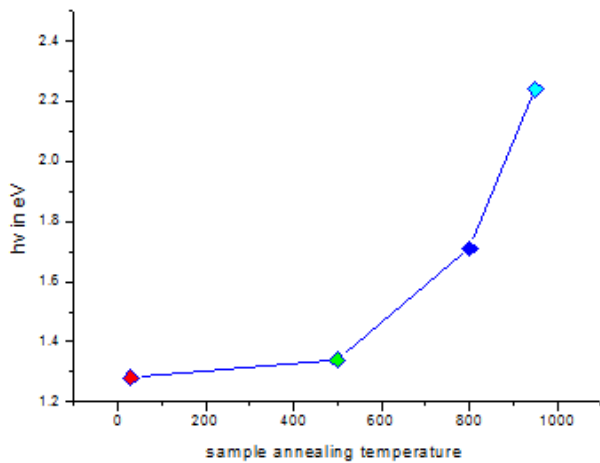


Figure 6: Band gap energy variation with the samples at varied annealing temperature of $\text{Fe}_2\text{Mn}_2\text{Ni}_2\text{Zn}_2\text{O}_{11}$

Due to an increase in temperature the crystallite size also increases which shows an increase in band gap energy [22]. The energy levels are dependent on the degree of structural order–disorder in the lattice. Therefore, the increase of structural organization in nano ceramic leads to a reduction of the intermediary energy levels and consequently increases the E_g values.

Tauc plot data well confirms that the band gap energy of the sample increases slightly when the temperature is increased.

A graph is drawn with natural logarithm of the absorption coefficient against energy in eV. (Figure 7). Urbach energy is calculated from this diagram. This value is found to be lower than the band gap energy and hence Sumi-Toyozawa(ST) model theory can be well applied to this material.

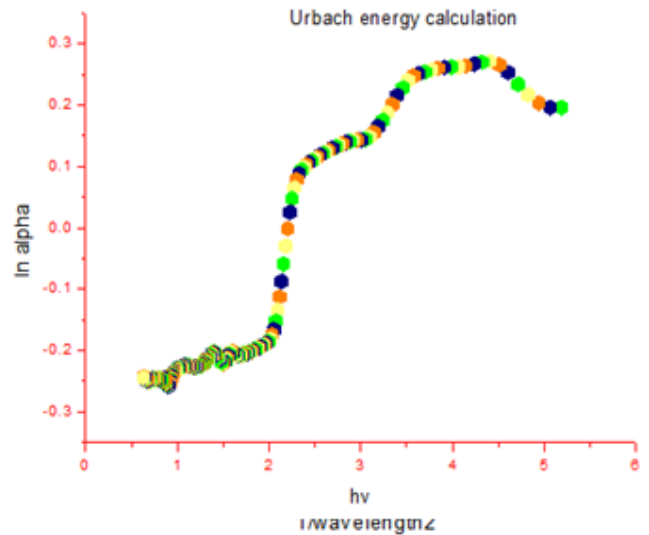
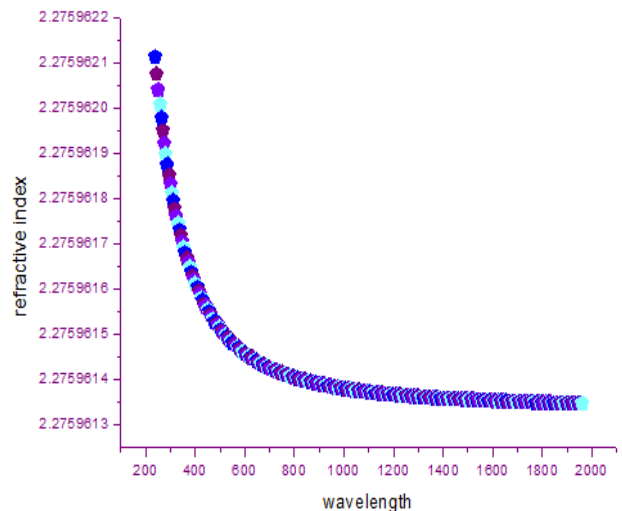


Figure 7: Absorption variation with photon energy of $\text{Fe}_2\text{Mn}_2\text{Ni}_2\text{Zn}_2\text{O}_{11}$

By the study of the variation of refractive index of the sample at different values of temperature, it is analyzed that refractive index of the sample decreases as the wavelength increases and attains a definite value at all temperatures. This linear variation of the refractive index with the wavelength is due to dispersion of light energy at the different interstitial layers. The refractive index of perovskites is known to be proportional to their electronic polarization per unit volume which is inversely proportional to distance. The refractive index also shows a linear relation with the photon energy (fig.8).The increase in refractive index is due to crystallization of the perovskite phase. This result can also be explained by an increase in crystallite size.



(a)

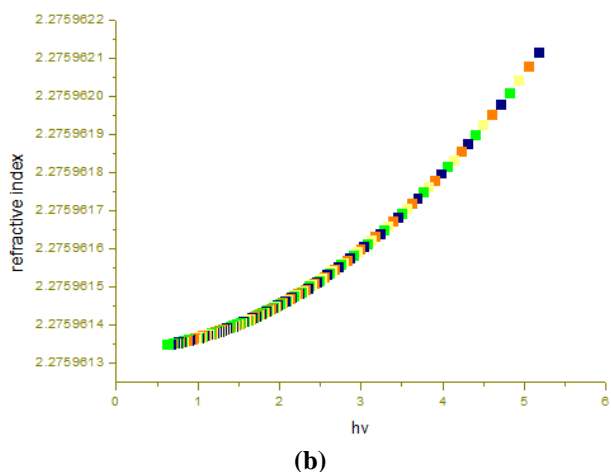


Figure 8: Variation of Refractive index (n) with (a) wavelength and (b) photon energy of Fe₂Mn₂Ni₂Zn₂O₁₁

The dispersion energy of the sample is calculated using the Wemple-DiDomenico (WD) model. Results are plotted graphically in (Fig.8). Refractive index of the sample annealed at different temperatures can be calculated using Sellmeier dispersion formula [23].

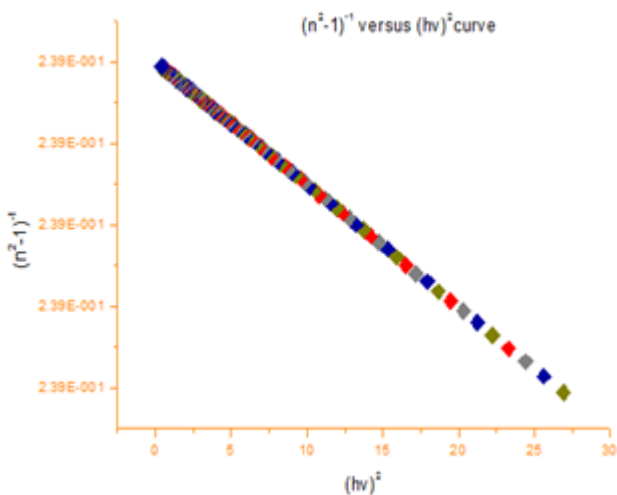


Figure 9: $(n^2-1)^{-1}$ versus $(hv)^2$ curve

Plotting of $(n^2-1)^{-1}$ against $(hv)^2$ allows to determine, the oscillator parameters, by fitting a linear function to the smaller energy data, E_o and E_d can be determined from the intercept, (E_o/E_d) and the slope $(1/E_oE_d)$. E_o is considered as an average energy gap to, it varies in proportion to the Tauc gap $E_o \sim 2E_g$. The data of the dispersion of the refractive index (n) were evaluated according to the single oscillator model proposed by Wemple and DiDomenico as, $n^2 = 1 + (E_dE_o)/(E_o^2-hv^2)$ ---- (7). Where E_o is the oscillator energy and E_d is the oscillator strength or dispersion energy.

The curves of $(n^2 - 1)^{-1}$ against $(1/\lambda^2)$ (Fig.10) are fitted into straight lines following the Sellmeier's dispersion formula. The value of S_o and (λ_o) are estimated from the slope $(1/S_o)$ and the infinite wavelength intercept $(1/S_o \lambda_o)^2$. The optical parameters of the sample were calculated and listed in the table.2 given below. The oscillator model can be also written as $n^2-1=S_o \lambda_o^2/[1-(\lambda_o/\lambda)^2]$ ---- (8) where λ is the wavelength

of the incident radiation, S_o is the average oscillator strength and λ_o is an average oscillator wavelength.

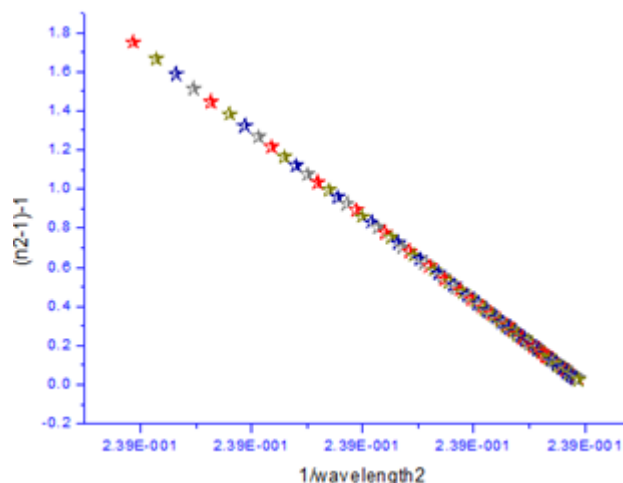


Figure 10: $(n^2-1)^{-1}$ versus $1/\lambda^2$ curve

Table 2: The calculated values of the optical parameters of Fe₂Mn₂Ni₂Zn₂O₁₁

Sample	E_g (eV)	E_o (eV)
At 30 ⁰	1.28	2.56
At 500 ⁰	2.34	4.68
At 800 ⁰	1.71	3.42
At 950 ⁰	2.24	4.48

From the above table it is clear that as the temperature is increased, band gap energy E_g and the oscillator energy E_o also increases. The dispersion energy also shows a decline as the temperature rises and the sample attains its perovskite phase. Further the mechano chemical process has an advantage due to low-costs and widely available materials, leading to a simplified process. The curves with straight line graphs confirm the Sellmeier's dispersion formula.

4. Conclusion

The increase in the band gap energy increases the dielectric properties of the material. The UV emission peak shifts significantly to higher wavelengths with increasing annealing temperatures. It is confirmed that tunable band gaps are obtained by varying annealing temperatures. Band gap energy and the optical properties of the nano ceramic material Fe₂Mn₂Ni₂Zn₂O₁₁ can be used for UV-VIS shielding applications. According to Wemple-DiDomenico single-oscillator model the dispersion energy decreases as the sample attains its perovskite phase. At high temperature the band gap energy increases and becomes more dielectric. For new generation capacitors nano crystalline ceramics Fe₂Mn₂Ni₂Zn₂O₁₁ materials will prove as a future substitute. Optical measurements confirmed that absorbance and reflectance increase with temperature.

5. Acknowledgement

The authors are thankful to SAIF, Kochi for providing the instrumental data, UGC for providing financial assistance, to the Principal, CMS College, Kottayam and Principal, DB college, Parumala, Kerala for providing the facilities.

References

- [1] Behnam Farid, research gate
- [2] N. Nepal, J. Li, M. L. Nakarmi, J. Y. Lin, and H. X. Jianga_ Temperature and compositional dependence of the energy band gap of AlGa_N alloys *Department of Physics, Kansas State University, Manhattan, Kansas 66506-2601*
- [3] Band gap From Wikipedia the free encyclopedia
- [4] Tauc plot From Wikipedia, the free encyclopedia
- [5] Anithasnair et al. Nano Trends: A Journal of Nanotechnology and Its Applications Volume 16, Issue 3, ISSN: 0973-418X
- [6] Vinila, V.S., Jacob, R., Mony, A., Nair, H.G., Issac, S., Rajan, S., Nair, A.S. and Isac, J. (2014) XRD Studies on Nano Crystalline Ceramic Superconductor PbSrCaCuO at Different Treating Temperatures. *Crystal Structure Theory and Applications*, **3**, 1-9. <http://dx.doi.org/10.4236/csta.2014>
- [7] Kumar et al. *International Nano Letters* 2013, 3:30
- [8] T Dhannia, S. Jayalekshmi, M. C. SanthoshKumar, T. PrasadaRao and A. ChandraBose, Effect of Aluminium
- [9] Doping and Annealing on Structural and Optical Properties of Cerium Oxide Nanocrystals, *Journal of Physics and Chemistry of Solids*, 70 (11), (2009) 1443 - 1447.
- [10] S. Varghese, M. Iype, E. J. Mathew and C. S. Menon, Determination of the Energy Band Gap of Thin Films of Cadmium Sulphide, Copper Phthalocyanine and Hybrid Cadmium Sulphide/Copper Phthalocyanine from Its Optical Studies, *Materials Letters*, 56 (6), (2002) 1078 - 1083.
- [11] Choudhury *et al. International Nano Letters* **2013**:25 doi:10.1186/2228-5326-3-25 licensee Springer
- [12] Keigo Suzuki, And Kazunori Kijima. 2005. Optical Band Gap Of Barium Titanate Nanoparticles Prepared By Rf-Plasma Chemical Vapor Deposition, *Japanese Journal of Applied Physics*, Vol. 44, No. 4a, 2005, Pp. 2081–2082, The Japan Society of Applied Physics.
- [13] Tauc, J., Menth, A., 1972 *Non Cryst. Solids* 569 8
- [14] S.Kugler –Lectures on Amorphous semiconductors
- [15] Dennis P. Shay -Development and characterization of high temperature, high energy density dielectric materials to establish routes towards power electronics capacitive devices- The Pennsylvania State University The Graduate School Department of Materials Science and Engineering May2014.
- [16] X.M Lu, J.S. Zhu, W.Y. Zang, G.Q. Ma, Y.N. Wang, *thin solid Films* 274 (1996) 165
- [17] N.Golego, S.A Studenikin, M. Cocivera, *Chem. Mater.* 10 (1998) 2000
- [18] M. Letz,¹ A. Gottwald,² M. Richter,² V. Liberman,³ and L. Parthier⁴ ¹Schott AG, Temperature-dependent Urbach tail measurements of lutetium aluminum garnet single crystal -Research and Development, Hattenbergstr. 10, D-55014 Mainz, Germany ²Physikalisch-Technische Bundesanstalt (PTB), Abbestr. 2-12, D-10587 Berlin, Germany ³Lincoln Laboratory, MIT, 244 Wood St., Lexington, Massachusetts 02420-9108, USA ⁴Schott Lithotec AG, Otto-Schott-Str. 13, D-07745 Jena, Germany--
PHYSICAL REVIEW B 81, 155109 _2010.
- [19] H. Sumi and Y. Toyozawa, *J. Phys. Soc. Jpn.* 31, 342 (1971).
- [20] S. Kugler: Lectures on Amorphous Semiconductors- 4 May 2013 ... www.slideserve.com/Leo/optical-properties
- [21] Tariq J. Alwan *Malaysian Polymer Journal*, Vol. 5, No. 2, p 204-213, 2010
- [22] Wug-Dong Park-- Optical Constants and Dispersion Parameters of CdS Thin Film Prepared by Chemical Bath Deposition *Electronic Materials and Devices Laboratory, Department of Railroad Drive and Control, Dongyang University, Yeongju 750-711, Korea* pISSN: 1229-7607 eISSN: 2092-7592.
- [23] Reenu Jacob, Harikrishnan G Nair, Jayakumari Isac- Optical band gap analysis of nano-crystalline ceramic PbSrCaCuO, *Journal of Advances in Physics*, 2014, ISSN 2347-3487.
- [24] M.J. DiDomenico, S.H. Wimple, *J. appl. Phys.* 40 919680 720.